PNPT1-mtRNA axis mediates chemotherapy-induced immune signaling and can be targeted to overcome therapeutic resistance

Supplementary information

Supplementary figure 1-7.

Supplementary Figure and Figure Legends

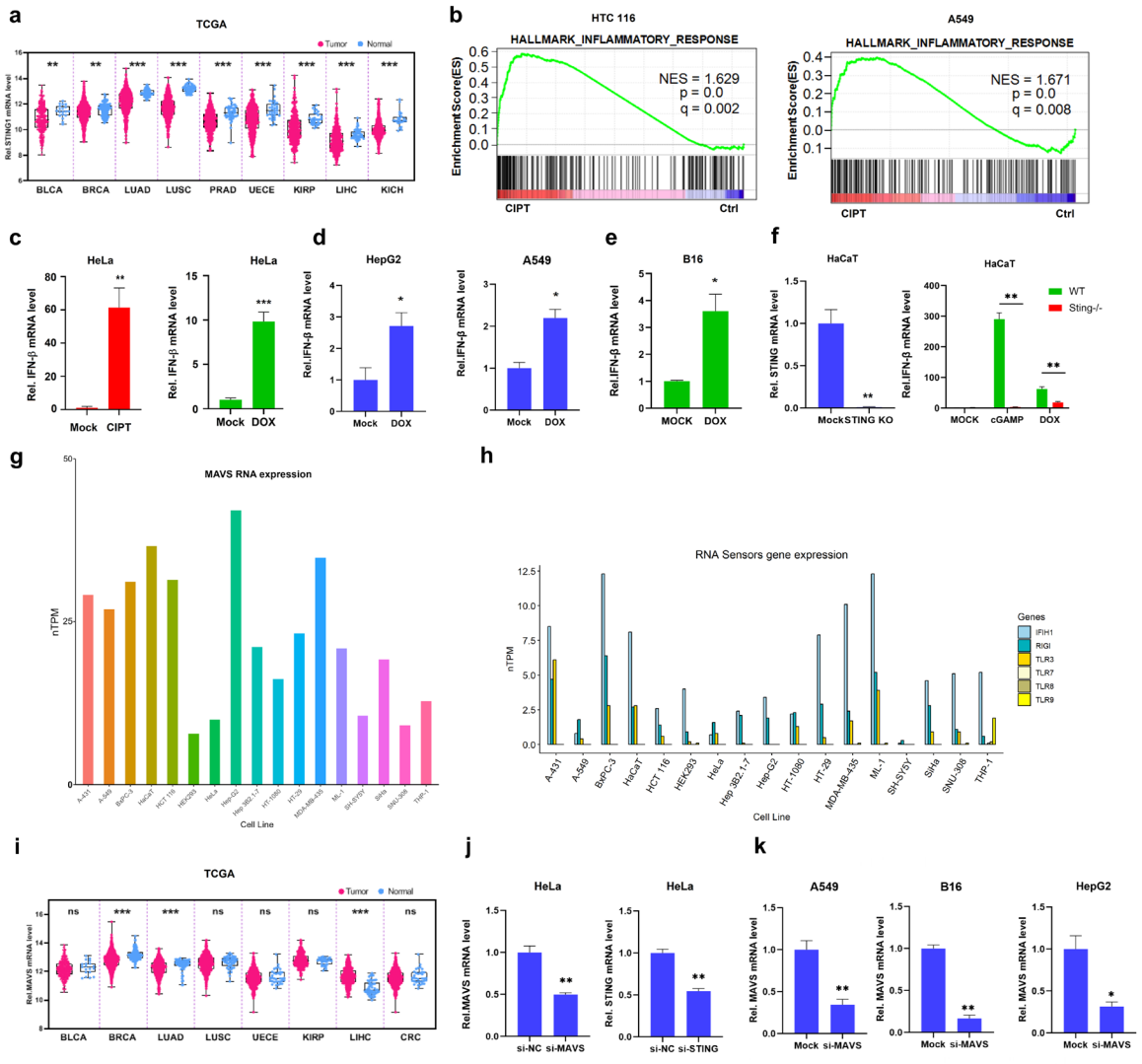

Fig S1. Chemotherapy induces immune responses

(a) STING expression in cancer and normal tissues was analyzed based on the TCGA dataset.

(b) GSEA plots show the enrichment of inflammatory response in human cancer cells following chemotherapy drug treatment in GSE235908 and GSE108214.

(c-e) Cells treated with different chemotherapy drugs for 12 hours were analyzed for IFN-β mRNA levels by RT-PCR.

(f) WT and STING knockout HaCaT cells treated with cGAMP and DOX, IFN-β mRNA were measured by RT-PCR.

(g, h) The bar chart shows the expression levels of MAVS and other nucleic acid receptors across different cell lines, with data sourced from the HPA database.

(i) MAVS expression in cancer and normal tissues was analyzed based on the TCGA dataset.

(j, k) Cells were transfected with small interfering RNA targeting STING, MAVS, or a negative control (Mock) for 24 hours, and the target genes were measured by RT-PCR.

Error bars are mean ± s.e.m. and are representative of 3 independent experiments. Statistical analyses were performed using Student's t-test, one-way ANOVA test with multiple comparisons, or Mann-Whitney U test; $*P < 0.05$.

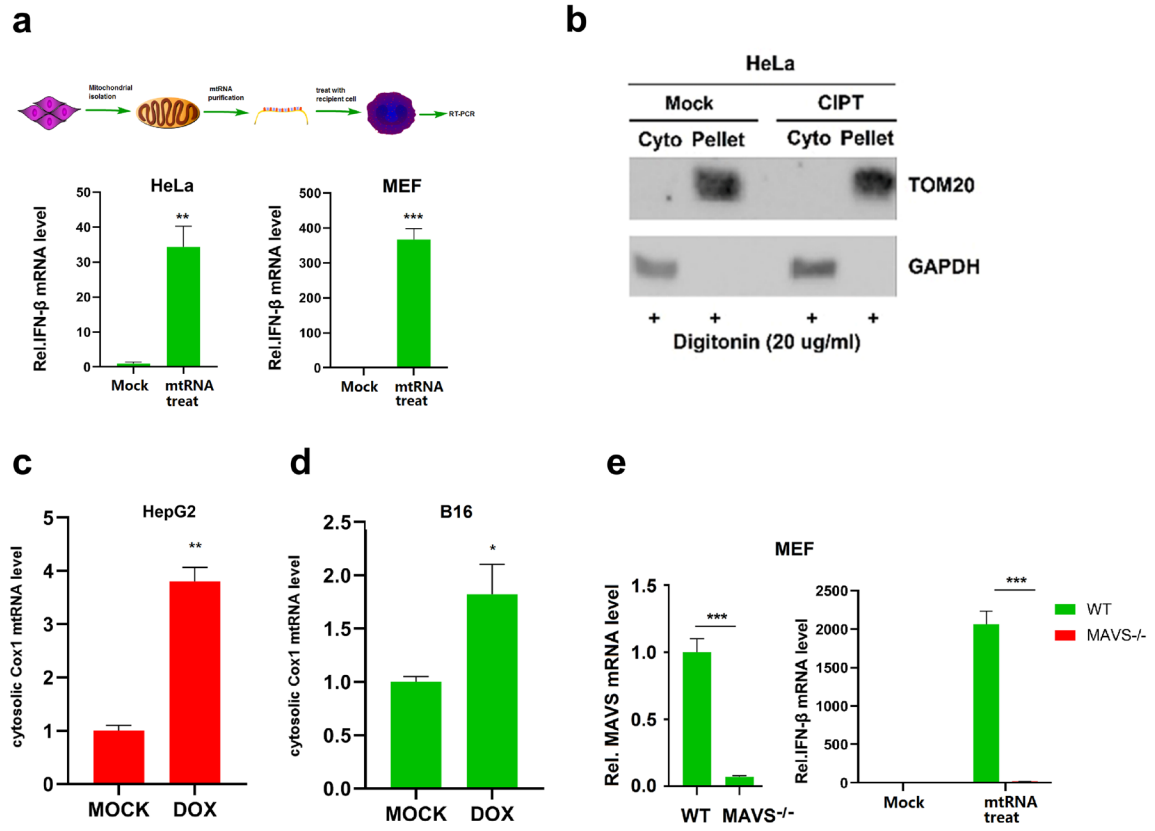

Fig S2. RNA recognition pathways are associated with anti-cancer immunity

(a) Top: A schematic diagram illustrating mtRNA and non-mtRNA purification and transfection; Bottom: mtRNA and non-mtRNA isolated from donor cells were transfected into recipient cells, and IFN-β mRNA levels were measured by RT-PCR.

(b) The purity of the cytosolic fraction was assessed using Western blotting.

(c, d) Both HepG2 and B16 cells were treated with DOX, and their cytosolic Cox1 mtRNA levels were measured by RT-PCR.

(e) WT mice and MAVS$^{-/-}$ mice MEFs were transfected with purified mtRNA, IFN-β mRNA was measured by RT-PCR.

Error bars are mean ± s.e.m. and are representative of 3 independent experiments. Statistical analyses were performed using Student's t-test or two-way ANOVA test with multiple comparisons; $*P < 0.05$

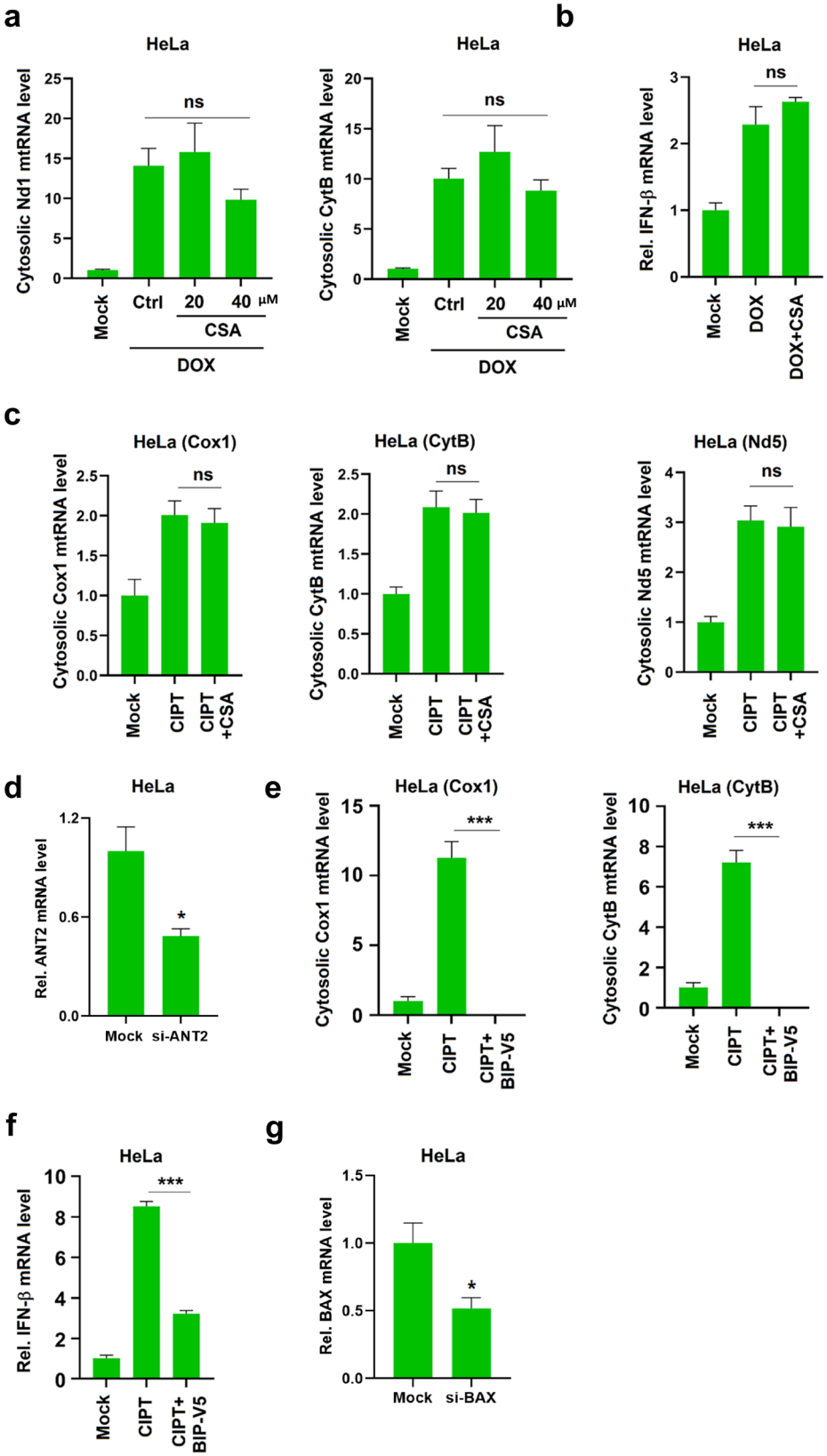
a
HeLa
Cytosolic Nd1 mtRNA level
ns
Mock
Ctrl
20
40 μM
CSA
DOX
HeLa
Cytosolic CytB mtRNA level
ns
Mock
Ctrl
20
40 μM
CSA
DOX
b
HeLa
Rel. IFN-β mRNA level
ns
Mock
DOX
DOX+CSA
c
HeLa (Cox1)
Cytosolic Cox1 mtRNA level
ns
Mock
CIPT
CIPT +CSA
HeLa (CytB)
Cytosolic CytB mtRNA level
ns
Mock
CIPT
CIPT +CSA
HeLa (Nd5)
Cytosolic Nd5 mtRNA level
ns
Mock
CIPT
CIPT +CSA
d
HeLa
Rel. ANT2 mRNA level
*
Mock
si-ANT2
e
HeLa (Cox1)
Cytosolic Cox1 mtRNA level
***
Mock
CIPT
CIPT+ BIP-V5
HeLa (CytB)
Cytosolic CytB mtRNA level
***
Mock
CIPT
CIPT+ BIP-V5
f
HeLa
Rel. IFN-β mRNA level
***
Mock
CIPT
CIPT+ BIP-V5
g
HeLa
Rel. BAX mRNA level
*
Mock
si-BAX

37

Fig S3. mtRNAs are released through the Bax pore

(a, b) HeLa cells were treated first with CSA and then with DOX, with cytosolic Nd1 and CytB mtRNAs measured by RT-PCR (**a**), and total IFN-β mRNAs assessed by RT-PCR (**b**).

(c) HeLa cells were treated first with CSA and then with CIPT. Cytosolic Cox1, CytB, and Nd1 mtRNAs were determined by RT-PCR.

(**d**) Cells were transfected with small interfering RNA targeting ANT2 or a negative control (Mock) for 24 hours, and the target gene was measured by RT-PCR.

(**e, f**) HeLa cells were treated first with BIP-V5 and then with CIPT for 12 h. Cytosolic Cox1 and CytB mtRNAs (**e**) and total IFN-β mRNA (**f**) were measured by RT-PCR.

(g) Cells were transfected with small interfering RNA targeting BAX or a negative control (Mock) for 24 hours, and the target gene was measured by RT-PCR.

Error bars are mean ± s.e.m. and are representative of 3 independent experiments. Statistical analyses were performed using Student's t-test or one-way ANOVA test with multiple comparisons; $*P < 0.05$.

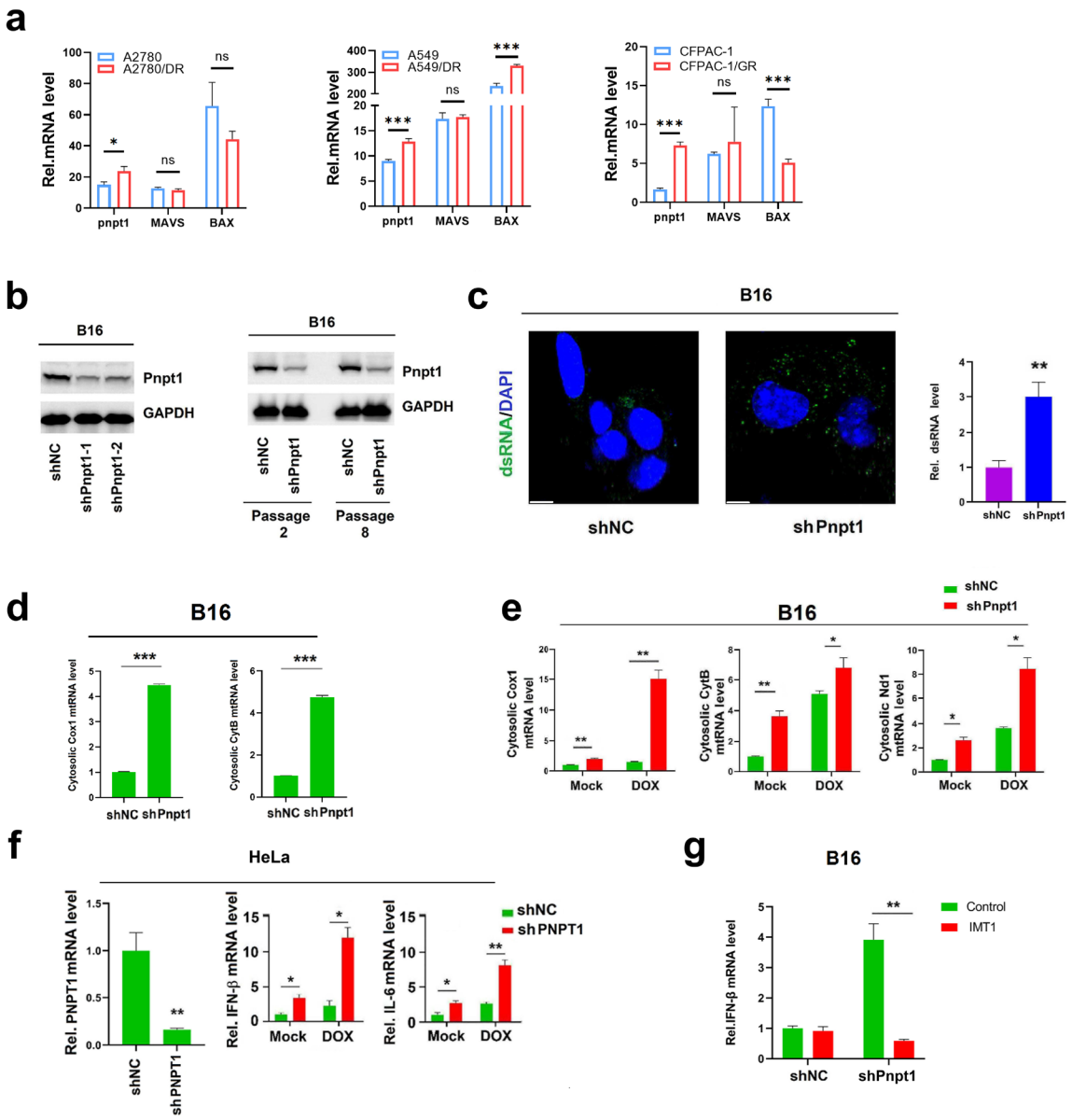

53

54 **Fig S4. PNPT1 Inhibits chemotherapy associated immune response**

55 **(a)** Bar chart showing the differences of the above genes between chemotherapy-sensitive

56 and insensitive cells, data from GEO datasets (GSE270030, GSE222187, GSE140077).

57 **(b)** B16 cells were treated with LV-shNC or LV-shPnpt1. PNPT1 protein was detected by

58 WB.

59 **(c)** Cellular dsRNA in B16 shNC or shPnpt1 cells were also detected by immunofluorescence

60 microscope. Scale bar = 20 μm

(d) Cytosolic mtRNA in B16 shNC or shPnpt1 cells were measured by RT-PCR.

(e) B16 shNC or shPnpt1 treated DOX. cytosolic mtRNA and were detected by RT-PCR.

(f) HeLa shNC or shPnpt1 treated DOX, Pnpt1, IFN-β and IL-6 mRNA were measured by RT-PCR.

(g) IFN-β mRNAs in B16 shNC or shPnpt1 cells were measured by RT-PCR after treatment with IMT1.

Error bars are mean ± s.e.m. and are representative of 3 independent experiments. Statistical analyses were performed using Student's t-test or two-way ANOVA test with multiple comparisons; $*P < 0.05$.

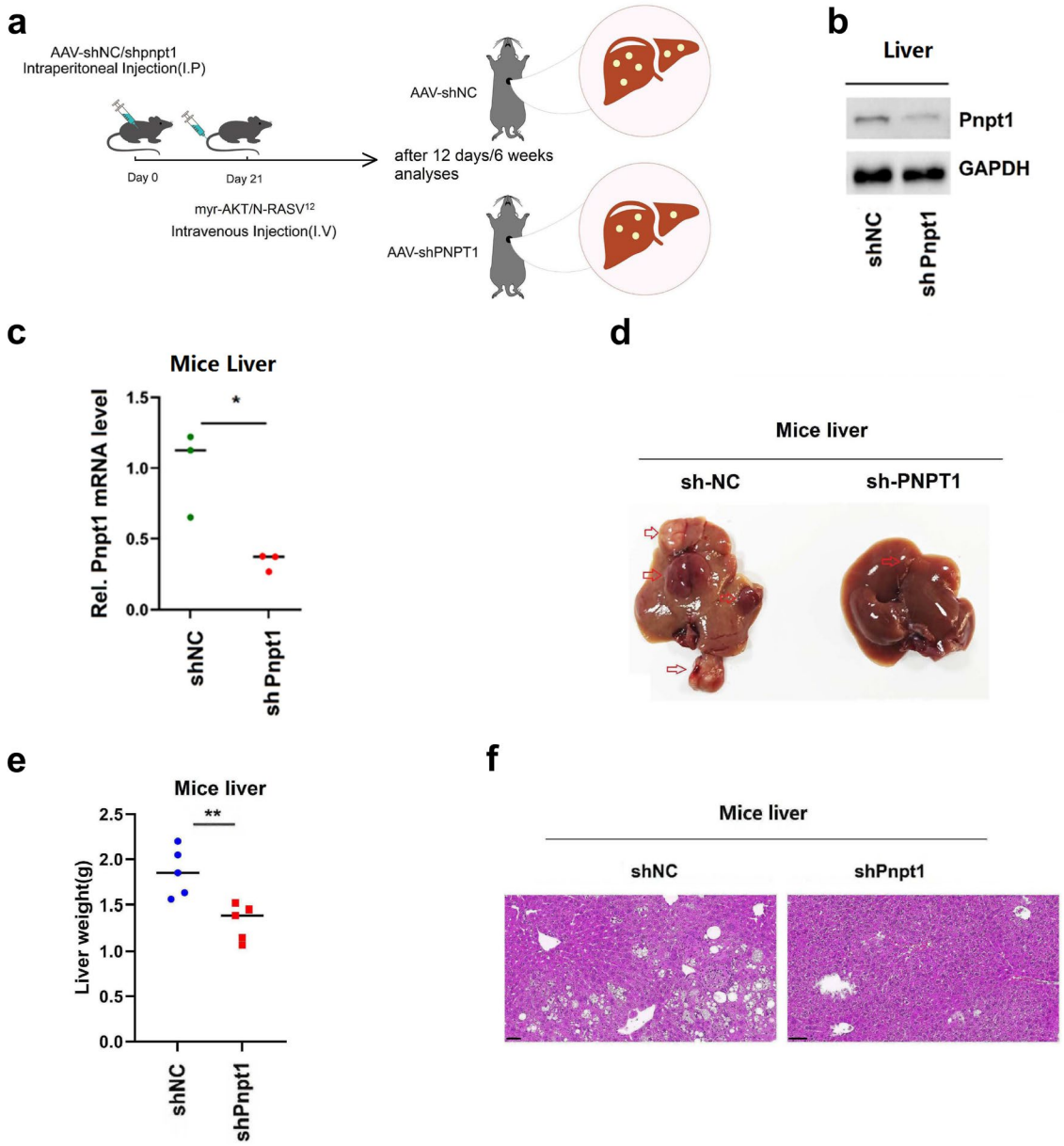

Fig S5. PNPT1 promotes primary liver cancer

(a) Experimental scheme for the injection of transposon-based vectors expressing myr-AKT and NRASV12 in mice.

(b, c) C57BL/6 mice (n = 3) were intraperitoneally injected with AAV expressing shPnpt1 (AAV-shPnpt1) or its control (AAV-shNC) for 3 weeks. Pnpt1 mRNAs in the mouse kidney and liver were measured by RT-PCR. PNPT1 protein was detected by WB.

(d-f) C57BL/6 control (shNC) and Pnpt1 knockdown (shPnpt1) mice underwent hydrodynamic injection of transposon-based vectors. After 6 weeks, liver tumor presentation (**d**), weight measurement (**e**), and H&E staining of the liver (**f**) were performed. Scale bar = 50 μm.

Error bars are mean ± s.e.m. and are representative of 3 independent experiments. Statistical analyses were performed using Student's t-test; $*P < 0.05$.

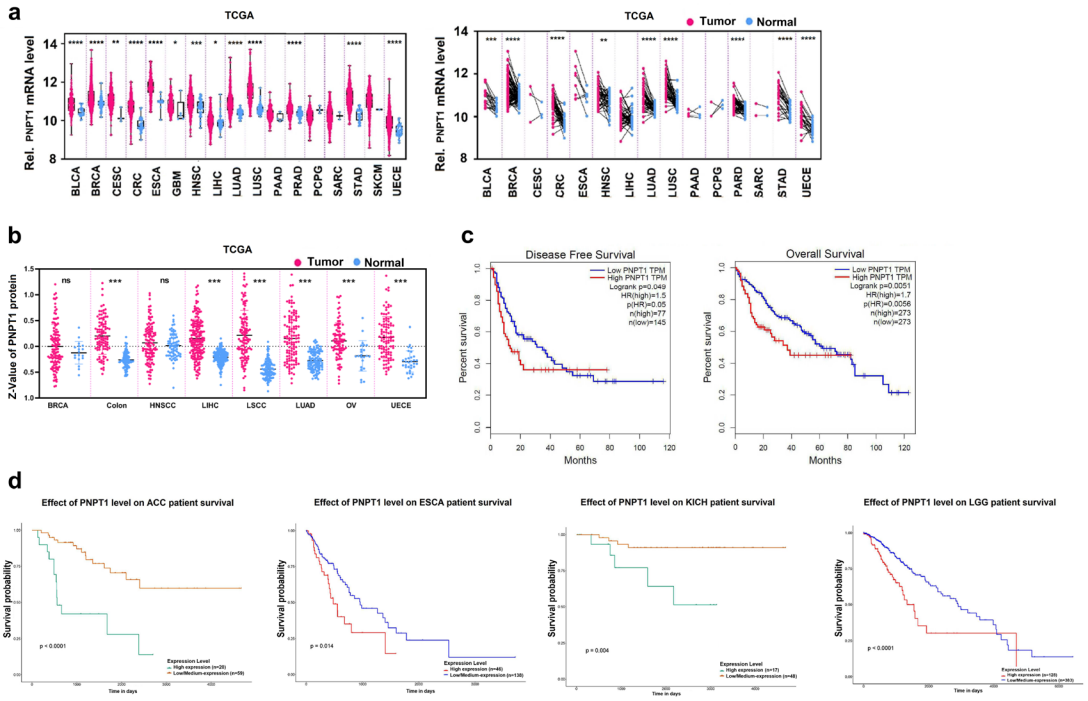

Fig S6. Tumor upregulation of PNPT1 promotes patient progression

(a, b) PNPT1 RNA and protein levels in cancer and normal tissues were analyzed based on the TCGA and CPTAC datasets.

(c) Kaplan-Meier curves showing overall survival and disease-free survival of human LIHC based on PNPT1 expression in LIHC tissues from GEPIA.

(d) UALCAN portal analyses (http://ualcan.path.uab.edu) examined the correlation between PNPT1 expression and survival rates in patients with adrenocortical carcinoma (ACC), esophageal carcinoma (ESCA), kidney chromophobe (KICH), and brain lower-grade glioma (LGG).

Error bars are mean ± s.e.m. and are representative of 3 independent experiments. Statistical analyses were performed using the Mann-Whitney U test or the Wilcoxon matched-pairs signed rank test; $*P < 0.05$.

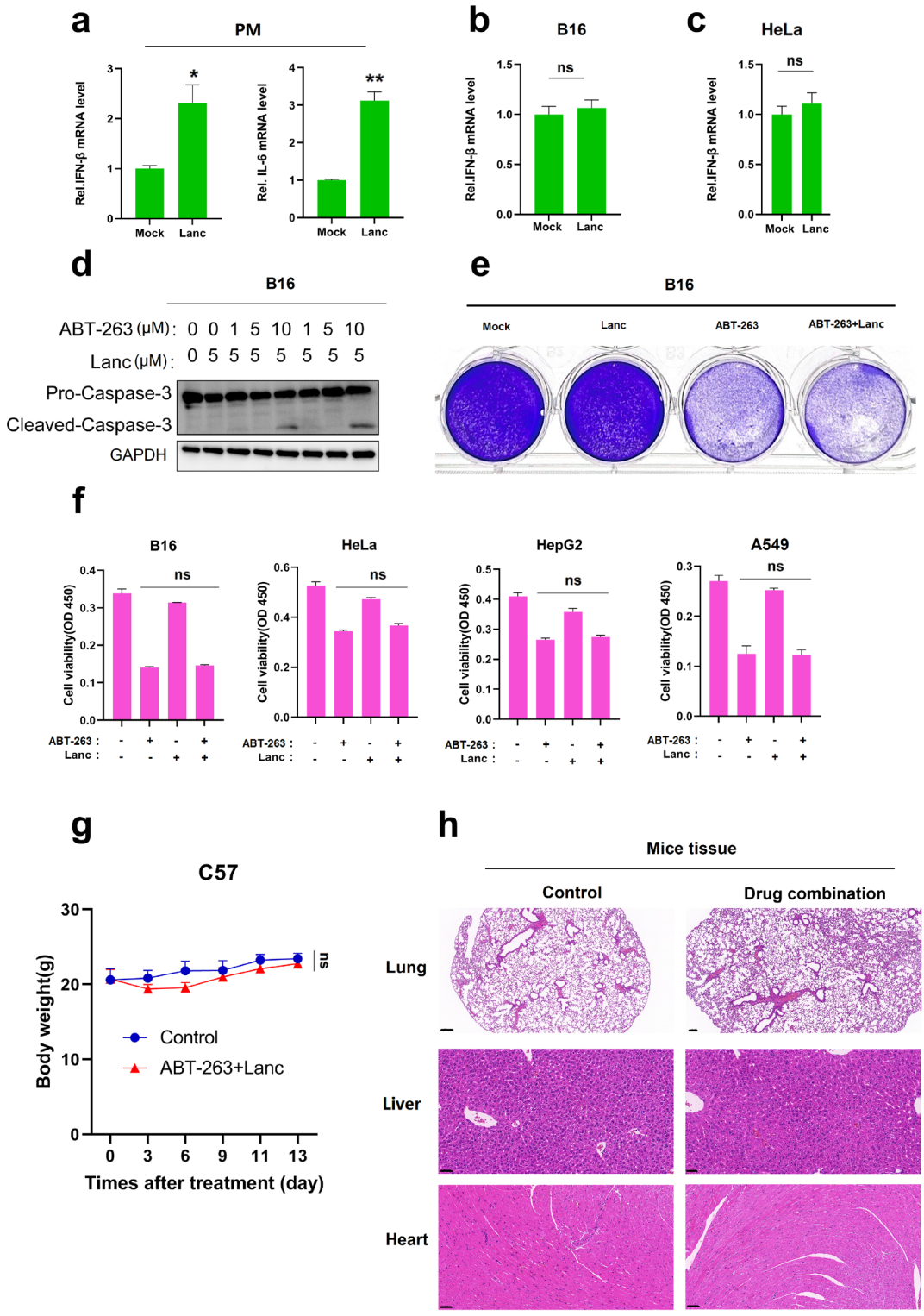

100

101 **Fig S7. Pharmacological inhibition of PNPT1 synergizes with BH3-mimetic drugs to**

102 **trigger anti-tumor immunity**

(a) PM cells were treated with Lanc (5 μM) for 12 hours, and IFN-β and IL-6 mRNA were measured by RT-PCR.

(b, c) B16 and HeLa cells were treated with Lanc (5 μM) for 12h, and IFN-β mRNA was measured by RT-PCR.

(d) B16 cells were treated with different combinations of drugs, and after 12h, activated caspase-3 was detected by WB.

(e) Clonogenic assay of B16 cells treated with different combinations of drugs.

(f) Cell viability assay of different cancer cell lines treated with drug combinations as indicated.

(g, h) C57BL/6 mice were treated with ABT-263 plus Lanc every three days until the end of the experiment (n = 5); mice body weight (**g**) was monitored, and H&E staining analyses of the liver, lung, and heart were conducted (**h**). Scale bar = 200 or 50 μm

Error bars are mean ± s.e.m. and are representative of 3 independent experiments. Statistical analyses were performed using Student's t-test, one-way ANOVA test with multiple comparisons, and two-way ANOVA test with multiple comparisons; $*P < 0.05$.